# Asynchronous haltere input drives specific wing and head movements in *Drosophila*

**Running title: Asynchronous haltere input**

Michael J Rauscher (mjr67@case.edu) and Jessica L Fox (jlf88@case.edu)

Case Western Reserve University Dept. Biology

**Keywords:**

Animal Behavior, Drosophila, Haltere, Insect Flight, Saccade, Multisensory Integration

## Abstract

Halteres are multifunctional mechanosensory organs unique to the true flies (Diptera). A set of reduced hindwings, the halteres beat at the same frequency as the lift-generating forewings and sense inertial forces via mechanosensory campaniform sensilla. Though it is well-established that haltere ablation makes stable flight impossible, the specific role of wing-synchronous input has not been established. Using small iron filings attached to the halteres of tethered flies and an alternating electromagnetic field, we experimentally decoupled the wings and halteres of flying *Drosophila* and observed the resulting changes in wingbeat amplitude and head orientation. We find that asynchronous haltere input results in fast saccades in the wing but not the head. We also find that wing and gaze optomotor responses are disrupted differently by asynchronous input. These effects of wing-asynchronous haltere input show that specific sensory information is necessary for maintaining wing amplitude stability and adaptive gaze control.

## Introduction

Animal locomotion, from crawling (Heckscher et al., 2015) to swimming (Wiggin et al., 2014) to walking (Wannier et al., 2001) to flight (Dickinson and Muijres, 2016), typically requires the coordinated motion of multiple body segments or appendages. Though this coordination can stem from the activity of a central pattern generator, sensory input from proprioceptors modulates body motions to adapt each step (Hiebert and Pearson, 1999; Noah et al., 2004). The specific contraction timing of muscles actuating multiple appendages can significantly change gait and posture, and thus the mechanisms ensuring limb coordination are essential to structuring adaptive locomotion.

In flying flies, proprioceptors on the wing (Dickinson, 1990) and haltere (Pringle, 1948) provide crucial feedback allowing for active control of each wingstroke to counteract flies' inherent pitch instability (Sun et al., 2007). The halteres are small club-shaped organs which have evolved from the hindwings of the true flies (Diptera). Long known to be required for stable flight (Derham, 1714), the halteres do not generate significant lift, but instead primarily detect inertial forces using campaniform sensilla at their base (Agrawal et al., 2017; Gnatzy et al., 1987; Pringle, 1948). Campaniform sensilla are a key class of insect proprioceptor, sensitive to strain forces acting on and within the cuticle (Chapman and Smith, 1963; Zill and Moran, 1981). Afferent neurons from haltere campaniform sensilla entrain their firing to a preferred phase of the haltere stroke cycle (Fox and Daniel, 2008; Yarger and Fox, 2018), which in *Drosophila* and most other fly taxa is biomechanically linked to the wing stroke cycle with an antiphase synchrony (Deora et al., 2015; Hall et al., 2015).

Continuous, stroke-synchronous feedback from the halteres is functionally important for wing-steering motoneurons and muscles (Dickerson et al., 2019; Heide, 1983; Pringle, 1948). In tethered flight, haltere ablation results in highly variable wing amplitudes and diminished wing optomotor responses (Bartussek and Lehmann, 2016; Dickinson, 1999; Mureli and Fox, 2015). The wing motoneurons are a primary target of haltere afferents, mediating a suite of compensatory equilibrium reflexes. In the blowfly *Calliphora*, some haltere afferents project directly to the motoneuron controlling the wing steering muscle wB1 (Fayyazuddin and Dickinson, 1996). Direct stimulation of the haltere nerve shows that it can entrain the firing of the wB1 motoneuron, which is normally more sensitive to reafference from the wing, if stimulation occurs within a specified time after the wing nerve's time of last firing (Fayyazuddin and Dickinson, 1999). In flying *Drosophila*, optogenetic manipulation of the haltere muscles

resets the firing phase of both the wB1 and wB2 muscles (Dickerson et al., 2019). What is the impact on the wings in flight if their motoneurons receive asynchronous haltere input? We hypothesize that the haltere's phase-locked input provides stabilizing input to the wing muscles, and that changing the phase of the haltere's stroke relative to the wing will result in wing amplitude instabilities.

Neck motoneurons also receive input from haltere afferents (Namiki et al., 2018; Strausfeld and Seyan, 1985), and mediate a similar suite of gaze-stabilizing reflexes (Hengstenberg et al., 1986). Following bilateral haltere ablation, flies are incapable of modulating the gain of optomotor gaze responses (Mureli et al., 2017). In recent work, we found that the head's movements are driven primarily by vision and not by the halteres (Rauscher and Fox, 2021). In larger flies, spiking responses to visual input are gated, but not modified, by haltere input in a subset of neck motoneurons: suprathreshold action potentials in these cells require haltere oscillation but are invariant to changes in haltere frequency (Huston and Krapp, 2009). We hypothesize that stroke-synchronous haltere information may be dispensable during visually-guided behaviors, with haltere input acting solely as a gating source of excitatory drive onto neck motoneurons. Under this hypothesis, we would expect both wing-synchronous and wing-asynchronous haltere input to be capable of modulating gaze optomotor behavior at similar or equivalent levels.

Previously, we showed that synchronous manipulation of the haltere's amplitude resulted in smooth changes in wingstroke amplitude and gaze direction (Rauscher and Fox, 2021). However, periods of smooth control over these kinematic outputs in fly flight are punctuated by abrupt changes in heading and gaze direction called saccades, analogous to the rapid stabilizing eye movements of vertebrates. These serve to minimize motion blur on the eyes and have been

extensively characterized in free flight (Land and Collett, 1974), tethered flight with free rotation about the yaw axis (Cellini and Mongeau, 2022; Land, 1973) and rigidly tethered flight (Cellini and Mongeau, 2020; Cellini et al., 2021; Kim et al., 2015). Saccades can occur spontaneously or be evoked by visual input, motivating study of the sensorimotor elements mediating saccades. Because saccades in tethered flight are larger and appear more frequently than saccades in free flight, their functional significance can be difficult to interpret. However, they are a distinct output of the wing and neck motor pathways, and observing how sensory modulation influences saccades can reveal pathways for processing sensory input. For example, Bender (2006) showed that changes to the bulb mass of the haltere (and thus the "gain" of the haltere's strain-sensitive campaniform sensilla) alters the dynamics of saccade termination for visually-initiated saccades.

To examine how haltere input drives smooth and saccadic wing and gaze behaviors, we experimentally decoupled the movement of the wings and haltere. By adding a small iron mass to one haltere, we immobilized it, abolishing it as a source of stroke-synchronous information. Then, using electromagnets, we drove the haltere at specific frequencies, moving it throughout its natural range of motion in a manner that was periodic and predictable but asynchronous with the wings. This movement allowed us to observe responses to wing-haltere phase relationships that do not naturally occur. We show that asynchronously-driven halteres increase the likelihood of saccadic steering changes in the wing motor output as well as the broadband noise levels of the wing's stroke amplitude. Movements of the head, by contrast, are not accompanied by an increase in broadband noise levels. However, the optomotor responses of both head and wings are significantly diminished by asynchronous haltere input. Our results show that synchronous haltere input is necessary for wing amplitude (but not gaze) stabilization and adaptive optomotor responses.

## Materials and Methods

*Animal care, haltere manipulations, and experimental trials*

Animals were reared from a colony of wild-caught *Drosophila melanogaster*. Adult female flies (aged 3-5 days post-eclosion) were cold-anaesthetized and attached to rigid tungsten pins using UV-curing dental cement. For magnetic stimulation experiments, a single iron filing was attached to the right haltere with UV-curing dental cement prior to tethering. Only iron filings of sufficient mass to immobilize the haltere with the magnets disengaged (filings in excess of 12μg, as determined in Rauscher and Fox, 2021) were used for experiments. For ablation experiments, one or both halteres were gently and completely removed using a pair of fine forceps.

Flies were given at least ten minutes to recover from haltere manipulation and tethering prior to usage in tethered flight behavioral experiments. Haltere stimulation periods lasted 3-4 seconds, which frequently evoked grooming of the haltere with the ipsilateral metathoracic leg. Time indices for grooming epochs were annotated manually and these video segments were excluded from analysis of head and wing kinematics. For filing-treated animals, successive presentations of different haltere stimulation conditions were preceded and followed by control epochs with the magnets disengaged lasting a minimum of 250ms (~50 wingbeats). For each animal, 1-6 epochs from the same experimental condition (from replicate stimulus presentations and intervening between grooming bouts) were drawn for subsequent analysis.

*Haltere stimulation*

To facilitate control over haltere stroke kinematics, two iron-core electromagnets were positioned anterior-dorsal and posterior-ventral to a tethered flying *Drosophila* (Fig. 1A). Each electromagnet was powered from a variable power supply (TP1803D, Tekpower, Montclair, CA, USA) switched through a power transistor (D1276A, Panasonic, Kadoma, Japan) and controlled via 5V TTL-level output from a data acquisition board (USB-6434, National Instruments, Austin TX, USA). Pulse trains consisted of 50% duty cycle square wave signals alternating at 25, 36, 50, 72, 100, or 167Hz. Signals sent to the two magnets were 180° out of phase with one another to produce a dorsal-ventral oscillation of the filing-treated haltere at the commanded frequency. Electromagnets were hand-wound using electromagnet wire and, as previously estimated (Rauscher and Fox, 2021), the field strength of each magnet was approximately 2000μT at the distance of the fly's body from the axial tip of each iron core (2mm).

*Visual stimulation*

To elicit optomotor responses, we used a wide-field vertical stripe pattern moving in the yaw aspect under the control of a 1Hz triangle wave, which was presented to the fly using a modular LED flight arena (Reiser and Dickinson, 2008). Stripes were one or two pixels wide and pseudo-randomly spaced such that average luminance of the wide-field panorama was 50%; i.e. the pattern consisted of an equivalent number of bright and dark pixels, where one pixel encompassed 3.75° of the circumference of the display (Fox et al., 2014). Different pattern velocities were achieved by varying the amplitude of the triangle wave whilst keeping the period constant.

*High-speed video and kinematic measurements*

Haltere and wing kinematics were recorded using two synchronized high-speed cameras (TS4 or IL5, Fastec Imaging, San Diego, CA, USA) with sagittal views of the fly from the left and right aspect. Recordings were made at 1000 or 2000fps for all treated animals and the majority of untreated animals, however some untreated animals were recorded at 750fps. In each video, the position of the haltere bulb was digitized using the DLTdv8 (Hedrick, 2008) or DeepLabCut (Mathis et al., 2018) software packages. Static points were manually labeled for each video at the position of the haltere base and anterior wing base. These were used to construct a common body-normalized coordinate framework for registering tracking data across animals, with the haltere base becoming the origin and the anterior wing base becoming coordinate (1,0). Wingbeat elevation time series were extracted using a custom MATLAB script. Haltere stroke amplitudes were estimated by measuring the range of each angular position time series. For asynchronously-driven trials, video segments shorter than the minimum period of a single cycle of the given frequency were excluded. A third camera recording at 100fps (Point Grey Chameleon3, FLIR, Wilsonville, OR, USA) provided a dorsal view used to measure head and wing kinematics. Head yaw with respect to the body axis and wing downstroke envelope kinematic time series were computed using a custom MATLAB program called Flyalyzer (https://github.com/michaelrauscher/flyalyzer), introduced previously in Rauscher and Fox, 2021. Shutter signals from each camera were recorded on the DAQ to facilitate alignment and synchronization of kinematic time series with one another and with the magnet control pulses and visual stimuli from the LED flight arena.

*Saccade detection and analysis*

Wing and head saccades were identified in kinematic traces from the 100fps camera using the amplitude (4° amplitude change in a single frame) and duration (10-100ms) thresholds described in Cellini et al., 2021. All detected saccades were used to calculate the saccade rates shown in Fig. 2C-E and Fig. 5C-D. For the saccade-triggered average (STA) responses shown in Fig. 2F-G (and Fig. S2B) as well as the stimulus-aligned cyclic average responses shown in Fig S2B-E, saccades were only included from 100fps video segments with concurrent high-speed tracking of the haltere and wingbeat on the lateral aspect cameras. Each 80ms saccade-triggered window used to produce the STA was baseline-subtracted and matched to a control window selected with a randomly drawn frame index from the same video segment. To produce the histograms shown in Fig. 3 and the heatmaps shown in Fig. S3, data were pooled from all available asynchronously-driven stimulus categories (up to and including 167Hz). Each frame from the 100fps camera was assigned a haltere position and wing instantaneous phase value at frame start by finding the single nearest-match frame recorded on the high-speed lateral aspect cameras (1000 or 2000 fps). Haltere angular velocity was computed as the numerical derivative of each haltere angular position time series. To assign a single angular velocity value to each frame from the 100fps camera, the root-mean-square value of the angular velocity time series was computed for all concurrent frames from the lateral aspect camera. Then, the sign (positive or negative) of the lateral aspect frame with the largest absolute value was applied to the result. A graphical summary of this process is included in Fig. S3A.

*Frequency-domain analyses*

For the estimation of broadband noise (Fig. S4), the fast Fourier transform (FFT) was calculated using only the first 150 samples of applicable kinematic time series from the dorsal-

view camera to provide a consistent spectral resolution of 0.67Hz. Time series were DC-leveled by fitting a least-squares regression line and then subtracting it out to remove linear trends. The area under the curve (AUC) of the resultant FFT was then estimated using the trapezoid method. For magnetic stimulation trials, we excluded a 4Hz range centered on the stimulus frequency from the AUC determination. For 50Hz trials, which were at the Nyquist limit for the dorsal view camera, an interval spanning 46-50Hz was instead excluded from the area under the curve measurement. For trials at frequencies exceeding the Nyquist limit for the dorsal view camera (72Hz, 100Hz, 167Hz), the excluded range encompassed the baseband alias of the driven haltere frequency. A range spanning 23-27Hz was excluded from trials without magnetic stimulation (untreated, haltere immobilized, single or double haltere ablation).

For estimation of visual response magnitude (Fig. 5), kinematic time series were DC-leveled as described above and zero-padded to 4096 samples. Magnitude estimates from resultant FFTs were then divided by the number of samples in each time series prior to zero-padding to normalize magnitudes for trials of varying length. Only segments longer than 64 samples were used, resulting in a coarsest possible spectral resolution of 1.5Hz.

## Results

### *Electromagnetic control of haltere stroke kinematics*

To establish magnetic control over one of the fly's two halteres, an iron filing was attached to the bulb (see Methods, Fig. 1A). With the electromagnets deactivated, this mass immobilized the haltere and prevented the fly from oscillating it. Activation of the electromagnets at 25, 36, 50, 72, 100, and 167 Hz resulted in movement of the haltere at the commanded frequency (Fig. 1B-F, Video S1). The natural oscillation of the halteres and wings

produces an out-of-phase relationship and commanding the haltere's frequency allowed us to sample wingbeats with all possible phase relationships. Haltere tracking data was registered into a unified coordinate framework, normalized using the haltere-thorax and wing-thorax joints as common control points, allowing us to survey movement of the haltere both within and in excess of its naturalistic range of motion (Fig 1C). In all observed trials, the untreated haltere maintained its full stroke amplitude (Fig. 1G). At the highest frequency tested, 13 out of 14 flies were unable to maintain a haltere amplitude that was within the range of those observed naturally (Fig 1G, 22 of 27 replicate trials). Because this commanded haltere motion was significantly smaller than those observed at lower frequencies, we excluded 167 Hz trials from further analyses that compared across conditions (see Methods). All conditions (save for the immobilized haltere) achieved peak angular velocities within the range of those observed in untreated animals (Fig 1H). Baseline wingbeat frequencies were statistically indistinguishable from untreated controls for all treatments (Fig. 1I), showing that our manipulations did not impair the gross functioning of the wing motor system.

*Asynchronous haltere movement evokes wing saccades*

Haltere primary afferents form synaptic connections with head- and wing-steering motoneurons either directly (Fayyazuddin and Dickinson, 1996; Fayyazuddin and Dickinson, 1999) or via interneurons (Strausfeld and Seyan, 1985; Trimarchi and Murphey, 1997). These thoracic microcircuits mediate a suite of compensatory equilibrium reflexes stabilizing the orientation of the body and head during flight (Dickinson, 1999; Sherman and Dickinson, 2003; Sherman and Dickinson, 2004). To investigate the impact of asynchronous haltere input on these

reflexes, we measured each animal's head yaw and wingstroke amplitudes (Fig. 2A, Video S2) using machine vision software developed previously in Rauscher and Fox, 2021.

We noted that treated flies showed significantly higher rates of wing saccades than the untreated control animals. Saccades in *Drosophila* and other flies are abrupt changes in heading, analogous to the optokinetic reflexes of vertebrates (Cellini and Mongeau, 2020; Cellini et al., 2021; Land, 1973; Land and Collett, 1974). In tethered flight, saccades appear as sharp changes in wing amplitude (Fig. 2B, Video S2). For each condition, we calculated the saccade rate (after Cellini et al., 2021) and found that all treatments exhibited higher ipsilateral wing saccade rates than untreated controls. Active asynchronous drive of the haltere at any frequency resulted in ipsilateral wing saccade rates comparable to those seen with bilateral haltere ablation, whereas haltere immobilization resulted in intermediate saccade rates comparable to those seen with unilateral ablation (Fig 2C). For contralateral wing saccades (Fig 2D), all treatment groups exhibited higher saccade rates than untreated control animals. In contrast, the head saccade rate was insensitive to haltere manipulation under all tested conditions save for bilateral ablation (Fig 2E), in agreement with previous findings that proprioceptive mechanosensory inputs, likely in the neck, are the primary driver of head saccades (Cellini et al., 2021).

*Haltere kinematic parameters influence saccade initiation*

In individual trials, fast Fourier transforms (FFTs) of wing and head kinematic time series (Fig S1) showed elevated spectral power at the magnetic stimulation frequency (or its baseband alias, for frequencies which exceeded the Nyquist limit of the camera measuring the wingstroke amplitude). Does the increased saccade rate explain the increase in power at the stimulation frequency? If halteres manipulations drive saccades, the saccade rate should increase with

increasing stimulus rate. Surprisingly, the average rate of ipsilateral wing saccades was uniform across magnetic stimulation frequencies, and that rate was indistinguishable from that seen with bilateral haltere ablation. Despite this, saccade-triggered average responses of the ipsilateral wing amplitude (Fig. 2F) and instantaneous wingbeat frequency (Fig. 2G) followed the frequency of the driving stimulus. As well, stimulus-triggered cyclic averages aligned on each magnetic stimulation pulse showed that saccade probability varied in time with the stimulus (Fig. S2A). Taken together, these data suggest that saccades occurred at specific times relative to the driving stimulus, but were not reliably elicited upon every stroke cycle. Saccades accompanying all haltere treatments were categorically of larger amplitude than those observed in untreated animals (Fig. S2B). Cyclic averages also illustrated that while the treated haltere's frequency and amplitude could be reliably commanded with the magnetic stimulation, the induced oscillation assumed a diversity of phase relationships with the magnetic stimulus across animals and between trials (Fig. S2C-E). This technical limitation implies that the timing of the stimulus could not necessarily predict the specific positions or phases of the haltere: these had to be measured directly from the high-speed video.

After observing phase-locked saccades, we sought to determine whether specific kinematic parameters of the haltere drove saccade initiation. Using all available high-speed frames, we assessed the haltere's angular position, angular velocity, and phase relationship to the wingstroke cycle (Fig 3A) and found that our manipulations resulted in values both within and outside of the range of values observed in untreated animals. This afforded the opportunity to observe responses to both naturally-occurring stimuli and stimuli that do not occur in flight.

We then created histograms assessing the probability of saccade initiation as a function of each kinematic parameter under each condition (Fig. 3B-C, Fig S3). Saccade probability was not

related to haltere angular position under any condition (Fig. 3B). Similarly, there was no relationship between the wing phase and the saccade probability under any condition (Fig. 3D). In untreated animals, the haltere's angular velocity was almost always high, whether the haltere was moving up or down (Fig. 3C, gray bars); in haltere-immobilized animals, the angular velocity was always low. Saccade probability was also low in these conditions, although higher than in untreated animals. When we drove the haltere in a velocity range either faster or slower than it's natural activity, however, we saw a dramatic increase in saccade probability (Fig. 3C, right). Multivariate probability heatmaps of multiple kinematic parameters did not reveal any trends over and above those outlined in univariate analysis (Fig. S3). Our data therefore show that flies respond to unnatural haltere velocities by initiating wing saccades, with little discernable influence from other measured kinematic parameters.

*Asynchronous haltere movement increases wingstroke amplitude variability*

Bilateral haltere ablation increases wingstroke amplitude variability (Dickinson, 1999; Mureli and Fox, 2015). Could the wing's amplitude stability be "rescued" with any periodic excitation from the halteres, or must this input be synchronous with the wings? Because variability in the time domain includes periodic input from the driven haltere (reflecting the saccadic steering changes discussed above), we estimated the broadband noise level in the frequency domain. This allowed us to estimate changes in the baseline amplitude variability, independent of the saccades, by measuring the area under the curve of the spectrum, excluding a narrow frequency band centered on the driven haltere frequency (see Methods, Fig. S5A-B).

Haltere immobilization increased the broadband noise in the ipsilateral wing amplitude (Fig. S5C) to a level comparable to that seen with unilateral ablation, whereas active

asynchronous drive using the electromagnets increased it further to levels equivalent to those seen with bilateral ablation. Similar responses of a smaller magnitude were observed for the contralateral wing (Fig. S5D), with all unilateral manipulations being distinct from those seen with untreated animals and bilateral ablation. Thus, not only does wing-asynchronous periodic input fail to stabilize the wing amplitude, it is categorically worse than no input at all. No haltere manipulation resulted in head yaw noise levels distinct from untreated animals, similar to our results when measuring saccade rate (Fig. S5E).

*Haltere-evoked saccades are not influenced by concurrent visual stimulation*

A major task of the fly thoracic nervous system is to integrate inertial sensory information from wingbeat-synchronous haltere afferents with descending information from the fly's motion vision system (Namiki et al., 2018; Namiki et al., 2022; Suver et al., 2016). Tethered flies adjust their gaze and wingstroke amplitude in response to widefield visual movement (Duistermars et al., 2007; Hengstenberg et al., 1986) acting through a motor pool shared with complementary reflexes driven by the halteres. This circuit architecture has been modeled as a "nested feedback" control system, in which "inner" feedback loops mediated by haltere-wing and haltere-head projections are hierarchically nested within an "outer loop" mediated by vision (Cellini and Mongeau, 2022; Schwyn et al., 2011). Within this framework, visual inputs can modulate haltere-mediated reflexes. We asked: does descending visual input influence wing saccades evoked by haltere stimulation?

Concurrently with each class of haltere treatment, we presented flies with a wide-field pattern of high-contrast vertical stripes moving at 1Hz in the yaw aspect with a pattern velocity of 90°/s (Fig. 4A-B,Video S3). We then subdivided each visual stimulus epoch into periods of

clockwise and anticlockwise visual motion (Fig. 4A-B) and calculated the saccade rate during each of these (as in Fig. 2). In both visual stimulus directions and for both wings, visual stimulation did not affect the saccade rate under the majority of haltere stimulus conditions (Fig. 4C-D). Notably, however, concurrent visual stimulation in either direction reduced the rate of ipsilateral wing saccades when the haltere was immobilized. For the contralateral wing, the saccade rate was significantly lower only for the anticlockwise direction, although the saccade rate in the clockwise condition was itself statistically indistinguishable from both the anticlockwise and uniform visual stimulus conditions. Our results suggest that descending visual input cannot "rescue" the wing from the destabilizing saccades resulting from asynchronous haltere input.

*Asynchronous haltere movement disrupts wing and head optomotor responses*

Halteres adjust the gain of wing and gaze optomotor equilibrium reflexes (Bartussek and Lehmann, 2016; Cellini and Mongeau, 2022; Mureli and Fox, 2015; Mureli et al., 2017; Rimniceanu et al., 2023). Is synchronous haltere input necessary for this function? To determine this, we estimated the optomotor response amplitude (following Rimniceanu et al., 2023) by measuring the magnitude of the FFT of each kinematic time series at 1Hz, the frequency of the visual stimulus (Fig. 5A-C). For the ipsilateral wing and head (Fig. 5D,F), all haltere manipulations resulted in categorically smaller visual response amplitudes than those seen in untreated flies. For the contralateral wing, only the bilateral ablation was statistically distinct from untreated animals (Fig. 5E).

Bilateral haltere ablation (as well as haltere immobilization) impairs the ability of flies to adjust their head responses to widefield visual stimuli, instead locking the fly into a fixed low-

amplitude response to all salient pattern velocities (Mureli et al., 2017). To assess the influence of our manipulations on optomotor tuning, we presented a subset of flies with a series of visual stimuli that moved at a range of pattern velocities spanning 30-240°/s. Untreated flies exhibited an optomotor tuning curve in response to these stimuli that peaked at 180°/s for wing responses (Fig. 5G-H) and 120°/s for head responses (Fig. 5I), in broad agreement with previous studies (Duistermars et al., 2007; Mureli et al., 2017). Similar tuning curves were observed for flies with immobilized halteres (Fig. 5G-I) although with significantly lower response amplitudes than the untreated flies (Fig. S5D). With the magnets engaged at 36Hz, optomotor tuning was abolished for both contralateral and ipsilateral wings. Visual pattern velocity was not a significant predictor of response amplitude for these flies (Fig 5G-H). In comparison, head responses showed lower gain relative to untreated controls, at levels comparable to those seen with haltere immobilization (Fig. 5I,S5C,F).

## Discussion

Coordinated motion of multiple appendages is so important that it is often very difficult to force them to move in uncoordinated ways. In flies, the biomechanics of the thorax restricts the halteres and wings to oscillate in perfect antiphase with no input from the nervous system: elevating the wing of a dead fly with forceps depresses the haltere (Deora et al., 2015). We used stimuli both within and outside the bounds of natural haltere motions to demonstrate the effects of asynchronous haltere perturbations on wing and head movements in flying flies. In previous studies, haltere ablation or immobilization was demonstrated to be deleterious to wing amplitude stability (Dickinson, 1999; Mureli and Fox, 2015) and optomotor reflexes (Bartussek and Lehmann, 2016; Mureli and Fox, 2015; Mureli et al., 2017), but these works left unresolved how

specific haltere information might contribute to each of these behavioral outputs. Consistent with our hypothesis that altering the phase of the haltere and wing should destabilize the wing motor output, our data demonstrate that both ipsilateral and contralateral wing steering reflexes are critically impaired by asynchronous haltere input, with increased saccades following "unnatural" haltere movements.

Though we hypothesized that haltere input of any kind would be sufficient for full-amplitude visually guided head movements, we instead observed that synchronous haltere input is necessary for attaining naturalistic levels of optomotor response gain. The head's movements, though receiving a more diverse set of inputs from both descending and ascending neurons and occurring at a lower speed, still shows deleterious effects of asynchronous haltere input. Asynchronous haltere input did not lead to higher rates of head saccades, congruent with previous findings showing that head saccades are primarily evoked by proprioceptive inputs to "reset" the head when it reaches the limits of its range of travel (Cellini et al., 2021).

*Asynchronous haltere input releases wing saccades, elevates wingstroke variability*

Our data show that asynchronous haltere input increases the saccade rate of the ipsilateral wing, and that these saccades are more likely when the haltere moves at angular velocities outside of its natural operating range. Experiments in which the entire body was rotated showed that the halteres are most sensitive to body angular velocity (Dickinson, 1999); our results extend this to show a relationship between the haltere's own angular velocity and movements of the wings. Are these saccades being driven by specific motions of the haltere? Our experiment with immobilized haltere suggests not: loss of one or both halteres also results in an elevated rate of saccades of similar amplitude. Therefore, another possible interpretation is that saccades emerge

spontaneously from the activity of the wing motor system, and that synchronous haltere input at specific haltere positions and velocities acts to suppress them.

This view accords well with our other finding that wingstroke amplitude variability also increases with the loss of input from one or both halteres in a stepwise fashion. This corroborates physiological recordings of the motoneuron controlling the first basalare muscle in *Calliphora* showing higher timing variability in spikes evoked by reafferent stimulation of the wing nerve as compared with those evoked by stimulation of the haltere nerve (Fayyazuddin and Dickinson, 1999). It is further corroborated by recent work in which behavior was recorded from the same individual flies under both a rigid body-fixed paradigm as well as a magnetic-suspension paradigm in which the body can rotate in the yaw plane (Rimniceanu et al., 2023). In the fixed condition, the wingstroke amplitude variability is categorically higher than when the same flies are freed to rotate about the yaw axis.

Campaniform sensilla are sensitive to compressive and shearing forces acting on and within the cuticle in which they are embedded (Chapman and Smith, 1963; Pringle, 1948; Zill and Moran, 1981). Such forces arise from the haltere's movement through its natural stroke plane and therefore scale proportionately with the bulb's angular velocity (Nalbach, 1993). As hypothesized by Pringle (1948) and predicted in subsequent modeling (Mohren et al., 2019), different fields of campaniform sensilla should also experience forces preferentially in-line with their receptive fields at different points within the stroke cycle. We might therefore predict that saccades are more or less likely to be initiated as a function of the haltere's angular position. Our results suggest that saccades may be slightly more likely when the asynchronously-driven haltere was in the downstroke position, but we did not observe a strong correspondence between haltere angular position and saccade initiation.

Though our data support the hypothesis that halteres suppress spontaneous saccades, rather than drive endogenous saccades, the extreme sensitivity of the campaniform sensilla forces us to consider the possibility that we were not able to stimulate or measure the haltere stimuli accurately enough to reach this conclusion. The firing properties of primary haltere afferents (Yarger and Fox, 2018) and downstream neck motoneurons (Haag et al., 2010)change significantly when the haltere oscillates naturally versus when its motion is driven exogenously, even in similar planes and frequencies. Additionally, our experimental setup was not optimized to measure all wingstroke parameters that have been shown to be relevant to steering output. While we have measured the peak downstroke angle of the wing as our proxy for steering effort, the total force produced by each wingstroke is a complex function of not just the downstroke angle, but also the wing joint deviation angle and the spanwise rotation angle of the wing (Muijres et al., 2015).

*Haltere influence on the contralateral wing*

In previous work (Rauscher and Fox, 2021), we manipulated the stroke amplitude of a beating haltere without compromising the haltere-wing stroke synchrony and evoked a consistent wing-steering response to the magnetic stimulation. Here, we found the response to haltere perturbation was less stereotyped and more probabilistic, but in neither the present nor previous work did we observe a clear relationship between the instantaneous wing phase and haltere-evoked changes in wing kinematic parameters. This was surprising given the organization of the wing-steering motor system downstream of haltere primary afferents, a major component of which are tonic muscles which fire once every stroke cycle and control muscle tension by varying their firing phase within it (Balint and Dickinson, 2001; Heide and Götz, 1996; Lindsay

et al., 2017; Tu and Dickinson, 1996). One possibility is that the haltere-evoked saccades in our data are mediated primarily by phasic muscles, for which the wing phase is comparatively less important for force generation. Another hypothesis is that the untreated opponent haltere (present in all of our manipulations) provides redundant input to contralateral wing motoneurons that can supersede an absent or malfunctioning ipsilateral haltere.

Our findings that asynchronous haltere input evokes wing saccades and increases the stroke amplitude variability of the contralateral wing are consistent with previous findings that each wing receives information from both halteres. Flies are capable of apparently normal flight following unilateral haltere ablation (Fraenkel, 1939). In *Calliphora*, input from a single haltere is sufficient to entrain the firing of the contralateral first basalare muscle following the ablation of the ipsilateral haltere and both wing nerves (Heide, 1983). Experiments rotating the fly's entire body showed that both amplitude and frequency components of haltere-wing reflexes are impaired following bilateral—but not unilateral—haltere ablation (Dickinson, 1999). Similar results were observed using a magnetic-suspension tethering system in which the fly initiated its own rotations: manipulating the bulb mass of a single haltere produced comparable changes in both clockwise and counterclockwise body saccades (Bender and Dickinson, 2006).

This bilateral integration implicates the contralateral haltere interneurons, or cHINs (Strausfeld and Seyan, 1985; Trimarchi and Murphey, 1997), which receive input from haltere afferents and represent the only known anatomical pathway through which haltere information crosses the body axis for both the wing and gaze motor control systems. Though anatomically conserved across fly taxa, these neurons have eluded physiological characterization to date, leaving many questions unresolved as to the sensory representations and transformations they mediate *en route* to their downstream motor targets. As we were unable to reliably elicit tethered

flight following any manipulation of both halteres aside from total bilateral ablation, behavioral explorations of this circuit's function are unlikely to be successful. Further exploration of each haltere's influence on the contralateral wing will likely remain contingent on a more complete description of the anatomy and physiology of haltere-wing thoracic microcircuits.

*Haltere contribution to head and wing optomotor responses*

As descending visual inputs concurrently target wing and gaze motoneurons (Chan et al., 1998; Namiki et al., 2018; Strausfeld and Seyan, 1985), we also examined multisensory integration of haltere and visual inputs. We show that haltere-wing asynchrony critically impairs the wing optomotor response to a degree comparable with bilateral haltere ablation. While this impairment may be unsurprising for wings, it is less obvious how the head might respond to asynchronous haltere input. Bilateral haltere ablation prevents flies from adjusting the gain of the head optomotor response to different pattern velocities (Mureli et al., 2017). Here, we show that loss of one haltere (by immobilization) or asynchronous input from one haltere reduces the optomotor response gain, but does not abolish pattern velocity tuning (Fig. 6).

In some of the neck motoneurons of quiescent *Calliphora*, an absence of haltere input prevents spiking responses to visual input, but spiking can be restored with haltere movement at any frequency, even as low as 10 Hz (Huston and Krapp, 2009). If the halteres are necessary only to provide flight-state-dependent excitatory drive onto the neck motor system, then asynchronous input would produce gaze optomotor tuning curves with similar or equivalent gain to an unmanipulated animal. Our data do not show this. Instead, we found that asynchronous drive of a single haltere resulted in head responses with lower gain. There are two main hypotheses that could explain why neck motoneurons that can be excited by asynchronous

haltere input in a quiescent state fail to produce high-gain visually-guided head movements when stimulated asynchronously in tethered flight.

First, the wing sensory inputs to the neck motoneurons are still unknown, raising the possibility that full neck motoneuron activity may require both wing and haltere input, like the wing motoneuron mnb1 (Fayyazuddin and Dickinson, 1996). This would allow the neck motoneurons to operate differently in flying and quiescent states. However, flies with ablated wings are still able to execute high-gain optomotor responses in tethered "flight" (thorax and halteres oscillating; Mureli et al., 2017) ). Though this would not preclude a role for wing reafference in head optomotor responses, as some mechanosensors (e.g. chordotonal organs at the base) may still function in the absence of wing aerodynamic loading, the complete wing sensory complement is unnecessary.

Second, the "control loop," in which descending neurons provide excitatory input to haltere muscles, (Chan et al., 1998; Dickerson et al., 2019) may explain this result. Our experiment breaks the control loop by nullifying the relationship between haltere muscle activity and haltere sensory input: visual input to the haltere muscles no longer produces haltere input that can be used to initiate proper reflexes. Both hypotheses could explain our results that visual input cannot "rescue" the wing from high noise and high saccade rates induced by haltere asynchrony (Fig. 4), and that visual tuning in the head remains intact but at lower gain. Future recordings of the electrophysiological properties of neck motoneurons under different behavioral conditions and of the haltere movement responses to visual inputs could help untangle these possibilities.

**Acknowledgments**

We would like to thank Chenxin Bi and Brandon Chun for help with data collection and annotation, as well as Noah DeFino, Jesse Fritz and Lauren Metz for fly care. We would also like to thank Hillel Chiel, Bradley Dickerson, Jeremiah Didion, Alexandra Gurgis, Nicholas Kathman, Kristianna Lea, Mark Willis, Gabriella Wolff, and Alexandra Yarger for helpful commentary.

## Competing interests

No competing interests declared.

## Funding

This work was supported by United States Air Force Office of Scientific Research [FA9550-14-0398 and FA9550-16-1-0165 to JLF]; and National Science Foundation [1754412 to JLF].

## Data Availability

All processed data is available in the associated Dryad repository. Raw video data available upon request. Kinematic time series for some untreated control animals in Figures 1-5 are included with a previously-published publicly available dataset (Rauscher and Fox, 2020).

## References Cited

**Agrawal, S., Grimaldi, D. and Fox, J. L.** (2017). Haltere morphology and campaniform sensilla arrangement across Diptera. *Arthropod Struct Dev* **46**, 215–229.

**Balint, C. N. and Dickinson, M. H.** (2001). The correlation between wing kinematics and steering muscle activity in the blowfly Calliphora vicina. *J Exp Biol* **204**, 4213–4226.

**Bartussek, J. and Lehmann, F.-O.** (2016). Proprioceptive feedback determines visuomotor gain in Drosophila. *R Soc Open Sci* **3**, 150562.

**Bender, J. A. and Dickinson, M. H.** (2006). A comparison of visual and haltere-mediated feedback in the control of body saccades in Drosophila melanogaster. *Journal of Experimental Biology* **209**, 4597–606.

**Cellini, B. and Mongeau, J. M.** (2020). Active vision shapes and coordinates flight motor responses in flies. *Proc Natl Acad Sci U S A* **117**, 23085–23095.

**Cellini, B. and Mongeau, J. M.** (2022). Nested mechanosensory feedback actively damps visually guided head movements in Drosophila. *Elife* **11**,.

**Cellini, B., Salem, W. and Mongeau, J. M.** (2021). Mechanisms of punctuated vision in fly flight. *Current Biology* **31**, 4009-4024.e3.

**Chan, W. P., Prete, F. and Dickinson, M. H.** (1998). Visual input to the efferent control system of a fly's "gyroscope". *Science* **280**, 289–292.

**Chapman, K. M. and Smith, R. S.** (1963). A linear transfer function underlying impulse frequency modulation in a cockroach mechanoreceptor. *Nature 1963 197:4868* **197**, 699–700.

**Deora, T., Singh, A. K. and Sane, S. P.** (2015). Biomechanical basis of wing and haltere coordination in flies. *Proc Natl Acad Sci U S A* **112**, 1481–6.

**Derham, W.** (1714). *Physico-theology: or, a demonstration of the being and attributes of God, from His works of creation. Being the substance of XVI sermons preached in St. Mary Le Bow-church, London, at the honble Mr. Boyle's lectures, in the years 1711 and 1712.* W. and J. Innys, London, 1714.

**Dickerson, B. H., de Souza, A. M., Huda, A. and Dickinson, M. H.** (2019). Flies regulate wing motion via active control of a dual-function gyroscope. *Current Biology* **29**, 3517–3524.

**Dickinson, M. H.** (1990). Comparison of encoding properties of campaniform sensilla on the fly wing. *Journal of Experimental Biology* **261**, 245–261.

**Dickinson, M. H.** (1999). Haltere-mediated equilibrium reflexes of the fruit fly, Drosophila melanogaster. *Philosophical Transactions of the Royal Society B: Biological Sciences* **354**, 903–916.

**Dickinson, M. H. and Muijres, F. T.** (2016). The aerodynamics and control of free flight maneuvers in Drosophila. *Philosophical transactions of the Royal Society of London B: Biological Sciences* **371**, 20150388.

**Duistermars, B. J., Reiser, M. B., Zhu, Y. and Frye, M. A.** (2007). Dynamic properties of large-field and small-field optomotor flight responses in Drosophila. *J Comp Physiol A Neuroethol Sens Neural Behav Physiol* **193**, 787–799.

**Fayyazuddin, A. and Dickinson, M. H.** (1996). Haltere afferents provide direct, electrotonic input to a steering motor neuron in the blowfly, Calliphora. *J Neurosci* **16**, 5225–5232.

**Fayyazuddin, a and Dickinson, M. H.** (1999). Convergent mechanosensory input structures the firing phase of a steering motor neuron in the blowfly, Calliphora. *J Neurophysiol* **82**, 1916–1926.

**Fox, J. L. and Daniel, T. L.** (2008). A neural basis for gyroscopic force measurement in the halteres of Holorusia. *J Comp Physiol A Neuroethol Sens Neural Behav Physiol* **194**, 887–897.

572 **Fraenkel, G.** (1939). The function of the halteres of flies (Diptera). *Proceedings of the Zoological Society*
573 *of London* **A109**, 69–78.

574 **Gnatzy, W., Grünert, U. and Bender, M.** (1987). Campaniform sensilla of Calliphora vicina (Insecta,
575 Diptera). *Zoomorphology* **106**, 312–319.

576 **Haag, J., Wertz, A. and Borst, A.** (2010). Central gating of fly optomotor response. *Pnas* **107**, 20104–
577 20109.

578 **Hall, J. M., McLoughlin, D. P., Kathman, N. D., Yarger, A. M., Mureli, S. and Fox, J. L.** (2015). Kinematic
579 diversity suggests expanded roles for fly halteres. *Biol Lett* **11**, 20150845.

580 **Heckscher, E. S., Zarin, A. A., Faumont, S., Clark, M. Q., Manning, L., Fushiki, A., Schneider-Mizell, C.**
581 **M., Fetter, R. D., Truman, J. W., Zwart, M. F., et al.** (2015). Even-skipped+ interneurons are core
582 components of a sensorimotor circuit that maintains left-right symmetric muscle contraction
583 amplitude. *Neuron* **88**, 314–329.

584 **Hedrick, T. L.** (2008). Software techniques for two- and three-dimensional kinematic measurements of
585 biological and biomimetic systems. *Bioinspir Biomim* **3**, 34001.

586 **Heide, G.** (1983). Neural mechanisms of flight control in Diptera. In *Biona-report 2* (ed. Fischer, G.), pp.
587 35–52. Stuttgart, New York.

588 **Heide, G. and Götz, K. G.** (1996). Optomotor control of course and altitude in Drosophila melanogaster
589 is correlated with distinct activities of at least three pairs of flight steering muscles. *Journal of*
590 *Experimental Biology* **199**, 1711–1726.

591 **Hengstenberg, R., Sandeman, D. C. and Hengstenberg, B.** (1986). Compensatory head roll in the blowfly
592 Calliphora during flight. *Proceedings of the Royal Society B: Biological Sciences* **227**, 455–482.

593 **Hiebert, G. W. and Pearson, K. G.** (1999). Contribution of sensory feedback to the generation of
594 extensor activity during walking in the decerebrate Cat. *J Neurophysiol* **81**, 758–70.

595 **Huston, S. J. and Krapp, H. G.** (2009). Nonlinear integration of visual and haltere inputs in fly neck motor
596 neurons. *Journal of Neuroscience* **29**, 13097–13105.

597 **Kim, A. J., Fitzgerald, J. K. and Maimon, G.** (2015). Cellular evidence for efference copy in Drosophila
598 visuomotor processing. *Nat Neurosci* **18**, 1247–1255.

599 **Land, M. F.** (1973). Head movement of flies during visually guided flight. *Nature 1973 243:5405* **243**,
600 299–300.

601 **Land, M. F. and Collett, T. S.** (1974). Chasing behaviour of houseflies (Fannia canicularis). *Journal of*
602 *comparative physiology 1974 89:4* **89**, 331–357.

603 **Lindsay, T., Sustar, A. and Dickinson, M. H.** (2017). The function and organization of the motor system
604 controlling flight maneuvers in flies. *Current Biology* **27**, 345–358.

605 **Mathis, A., Mamidanna, P., Cury, K. M., Abe, T., Murthy, V. N., Mathis, M. W. and Bethge, M.** (2018).
606 DeepLabCut: markerless pose estimation of user-defined body parts with deep learning. *Nat*
607 *Neurosci* **21**, 1281–1289.

**Mohren, T. L., Daniel, T. L., Eberle, A. L., Reinhall, P. G. and Fox, J. L.** (2019). Coriolis and centrifugal forces drive haltere deformations and influence spike timing. *J R Soc Interface* **16**, 20190035.

**Muijres, F. T., Elzinga, M. J., Iwasaki, N. A. and Dickinson, M. H.** (2015). Body saccades of Drosophila consist of stereotyped banked turns. *Journal of Experimental Biology* **218**, 864–875.

**Mureli, S. and Fox, J. L.** (2015). Haltere mechanosensory influence on tethered flight behavior in Drosophila. *Journal of Experimental Biology* 2528–2537.

**Mureli, S., Thanigaivelan, I., Schaffer, M. L. and Fox, J. L.** (2017). Cross-modal influence of mechanosensory input on gaze responses to visual motion in Drosophila. *Journal of Experimental Biology* **220**, 2218–2227.

**Nalbach, G.** (1993). The halteres of the blowfly Calliphora. *Journal of Comparative Physiology A* **173**, 293–300.

**Namiki, S., Dickinson, M. H., Wong, A. M., Korff, W. and Card, G. M.** (2018). The functional organization of descending sensory-motor pathways in drosophila. *Elife* **7**, e34272.

**Namiki, S., Ros, I. G., Morrow, C., Rowell, W. J., Card, G. M., Korff, W. and Dickinson, M. H.** (2022). A population of descending neurons that regulates the flight motor of Drosophila. *Current Biology* **32**, 1–8.

**Noah, J. A., Quimby, L., Frazier, S. F. and Zill, S. N.** (2004). Walking on a “peg leg”: Extensor muscle activities and sensory feedback after distal leg denervation in cockroaches. *J Comp Physiol A Neuroethol Sens Neural Behav Physiol* **190**, 217–231.

**Pringle, J. W. S.** (1948). The gyroscopic mechanism of the halteres of Diptera. *Philosophical Transactions of the Royal Society B: Biological Sciences* **233**, 347–384.

**Rauscher, M. J. and Fox, J. L.** (2020). Weighted haltere and imposed haltere stroke reduction tethered flying Drosophila kinematics. *Dryad, Dataset*.

**Rauscher, M. J. and Fox, J. L.** (2021). Haltere and visual sensory inputs sum linearly to predict wing (but not head) motor output in tethered flying Drosophila. *Proceedings of the Royal Society B* **288**, 20202374.

**Reiser, M. B. and Dickinson, M. H.** (2008). A modular display system for insect behavioral neuroscience. *J Neurosci Methods* **167**, 127–139.

**Rimniceanu, M., Currea, J. P. and Frye, M. A.** (2023). Proprioception gates visual object fixation in flying flies. *Current Biology* **33**, 1459-1471.e3.

**Schwyn, D. A., Heras, F. J. H., Bolliger, G., Parsons, M. M., Krapp, H. G. and Tanaka, R. J.** (2011). Interplay between feedback and feedforward control in fly gaze stabilization. *IFAC Proceedings Volumes (IFAC-PapersOnline)* **18**, 9674–9679.

**Sherman, A. and Dickinson, M. H.** (2003). A comparison of visual and haltere-mediated equilibrium reflexes in the fruit fly Drosophila melanogaster. *Journal of Experimental Biology* **206**, 295–302.

**Sherman, A. and Dickinson, M. H.** (2004). Summation of visual and mechanosensory feedback in Drosophila flight control. *Journal of Experimental Biology* **207**, 133–142.

**Strausfeld, N. J. and Seyan, H. S.** (1985). Convergence of visual, haltere, and prosternal inputs at neck motor neurons of Calliphora erythrocephala. *Cell Tissue Res* **240**, 601–615.

**Sun, M., Wang, J., Xiong, Y., Sun, M., Wang, J. and Xiong, Y.** (2007). Dynamic flight stability of hovering insects. *Acta Mech Sin* **23**, 231–246.

**Suver, M. P., Huda, A., Iwasaki, N., Safarik, S. and Dickinson, M. H.** (2016). An array of descending visual interneurons encoding self-motion in Drosophila. *The Journal of Neuroscience* **36**, 11768–11780.

**Trimarchi, J. R. and Murphey, R. K.** (1997). The shaking-B2 mutation disrupts electrical synapses in a flight circuit in adult Drosophila. *Journal of Neuroscience* **17**, 4700–4710.

**Tu, M. S. and Dickinson, M. H.** (1996). The control of wing kinematics by two steering muscles of the blowfly (Calliphora vicina). *Journal of Comparative Physiology A 1996 178:6* **178**, 813–830.

**Wannier, T., Bastiaanse, C., Colombo, G. and Dietz, V.** (2001). Arm to leg coordination in humans during walking, creeping and swimming activities. *Experimental Brain Research 2001 141:3* **141**, 375–379.

**Wiggin, T. D., Peck, J. H. and Masino, M. A.** (2014). Coordination of fictive motor activity in the larval zebrafish is generated by non-segmental mechanisms. *PLoS One* **9**, e109117.

**Yarger, A. M. and Fox, J. L.** (2018). Single mechanosensory neurons encode lateral displacements using precise spike timing and thresholds. *Proceedings of the Royal Society B: Biological Sciences* **285**, 20181759.

**Zill, S. N. and Moran, D. T.** (1981). The exoskeleton and insect proprioception. I. Responses of tibial campaniform sensilla to external and muscle-generated forces in the American cockroach, Periplaneta americana. *Journal of Experimental Biology* **91**, 1–24.

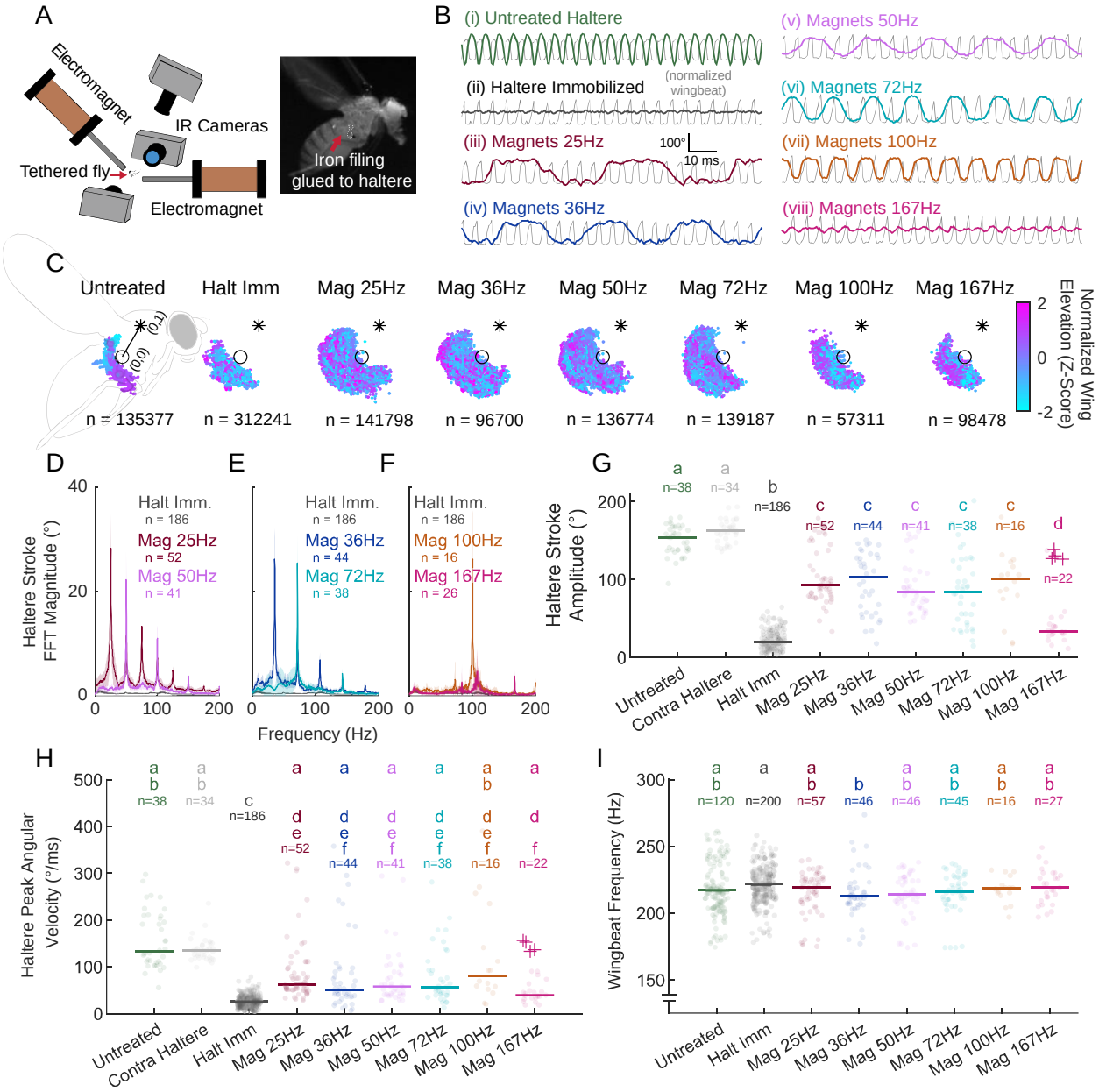


**Figure 1. Electromagnetic control of haltere movement asynchronous from the wings.** **(A)** Schematic of iron filing treatment (top, inset) and electromagnetic stimulation system (bottom). **(B)** Representative traces showing movement of untreated haltere at wingbeat frequency (~200Hz), immobilized haltere treated with iron filing (ii), and actively-driven haltere at a range of frequencies controlled by electromagnets (iii-viii) **(C)** Haltere tracking by condition, registered into a normalized body coordinate system defining the haltere base as the origin, represented by circle and the anterior wing base as (0,1), represented by asterisk. Colors reflect the z-normalized wingstroke elevation at each measurement point. **(D)** Mean FFT (95% confidence interval shaded) of all high-speed (1000 or 2000fps) time series with the haltere immobilized (black), driven at 25Hz (red), and 50Hz (pink). **(E)** same as (D) for 36Hz (blue) and 72Hz (teal) frequencies. **(F)** same as (D) and (E) for 100Hz (orange) and 167Hz (magenta) frequencies. **(G-I)** Haltere stroke amplitude (G), peak angular velocity (H) and baseline wingbeat frequencies (I) observed under each haltere manipulation. Lines show median for each group. 167Hz responses from outlier animal shown with +. Letters denote statistical groupings from multiple Bonferroni-corrected Wilcoxon rank-sum test (5% alpha).

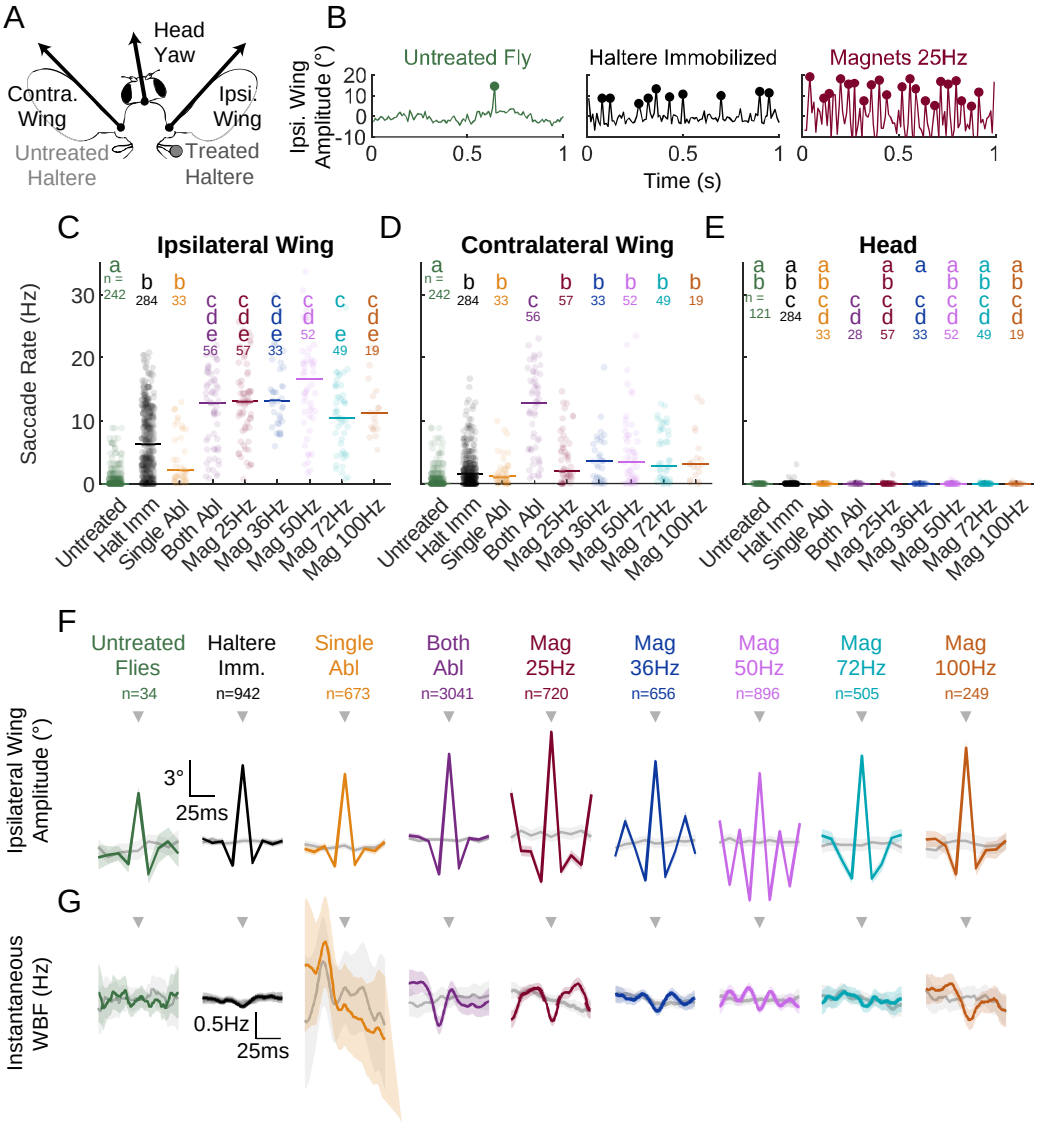


**Figure 2. Haltere manipulation increases saccade rate in kinematic outputs downstream of halteres.** **(A).** Schematic of measured kinematic outputs, recorded at 100fps, showing downstroke amplitude (angle of wing envelope leading edge) for each wing and yaw movement of the head. **(B)** Example ipsilateral wing amplitude traces under haltere treatment conditions. Positive-going angles denote counterclockwise changes in the projected wing envelope leading edge angle which for the right-hand wing (as in all depicted examples) signifies an increase in downstroke amplitude. **(C)** Ipsilateral wing saccade rates from all haltere treatments (see Methods). Left and right wing responses for symmetrical manipulations (untreated, bilateral ablation) are pooled. Lines show median for each group. Letters denote statistical groupings from multiple Bonferroni-corrected Wilcoxon rank-sum test (5% alpha). **(D,E)** Same as (C) for contralateral wing and head saccade rates, respectively. **(F)** Saccade-triggered average ipsilateral wing amplitude responses for each condition (Shade, 95% confidence interval). Gray triangles show the saccade peak, around which each constitutive video segment of the STA is indexed. Gray traces show controls triggered from random indices within the same time series. **(G)** Same as (F) but for the baseline-subtracted instantaneous wingbreat frequency.

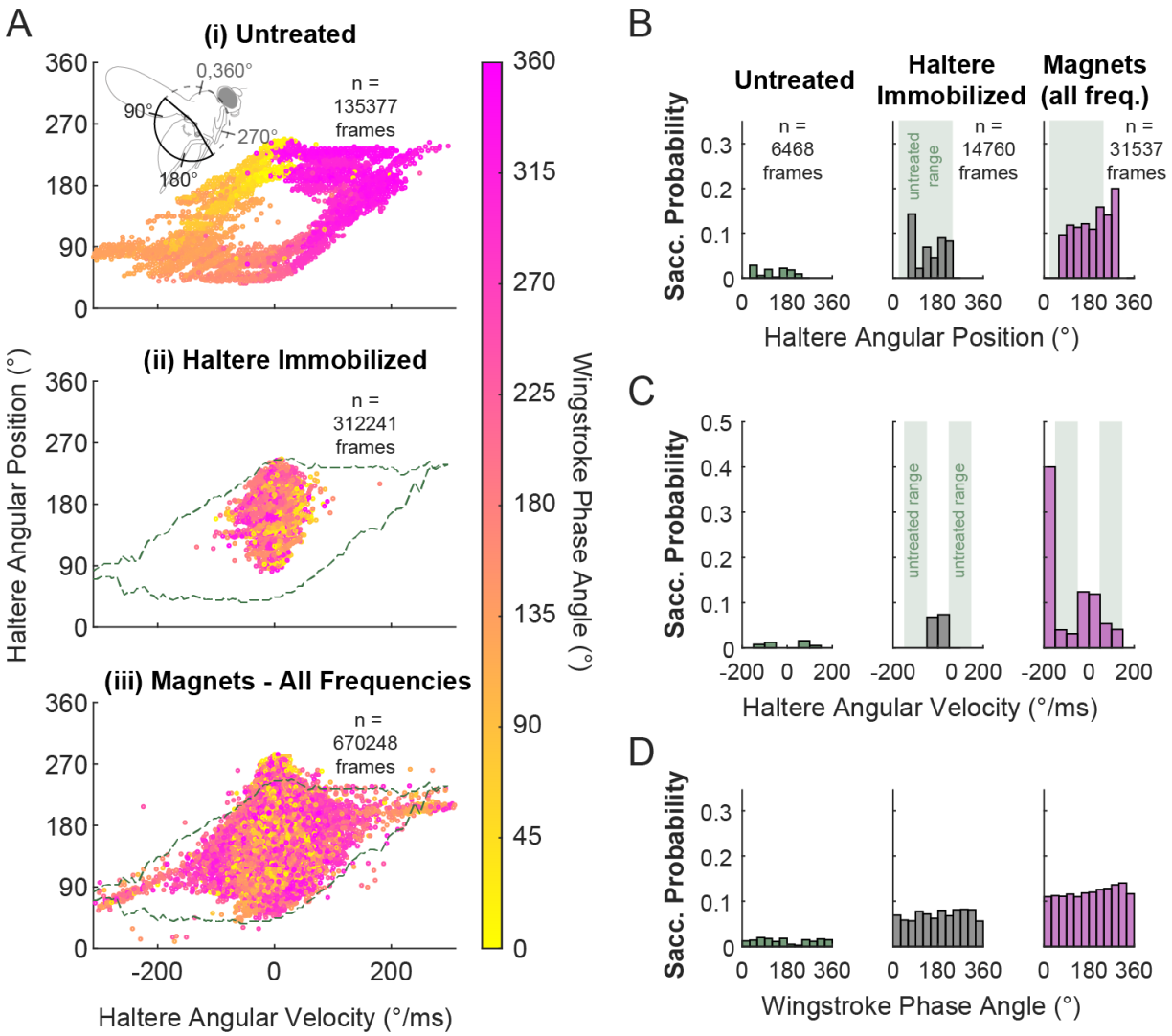


**Figure 3. Ipsilateral wing saccades are more likely when the haltere exceeds normal kinematic parameters** **(A)** Summary of haltere angular position, angular velocity, and wing instantaneous phase from all high speed data, separated by condition. (Ai) Untreated animals, showing natural antiphase synchrony of haltere and wings. Inset shows unified body coordinate scheme, with haltere upstrokes typically occupying the 45-90° range and downstrokes typically occupying the 235-270° range (Aii) Frames from haltere immobilized (magnets OFF) condition. Green dashed line shows extent of the naturalistic parameter space observed in the untreated animal. (Aiii) High-speed frames aggregated from all magnetic stimulation frequencies, showing broad overlap with the naturalistic range of haltere angular velocities and angular positions. **(B)** Histograms of ipsilateral wing amplitude video frames showing probability of saccade as a function of haltere angular position at frame onset for each condition. Light green shaded region outlines the natural range of haltere angular positions **(C).** Same as (B) but for haltere signed-RMS angular velocity throughout the frame (see Methods). Light green shaded regions outline the naturalistic range of negative (upstroke) and positive (downstroke) angular velocities. **(D)**. Same as (B) but for wing instantaneous phase at frame onset.

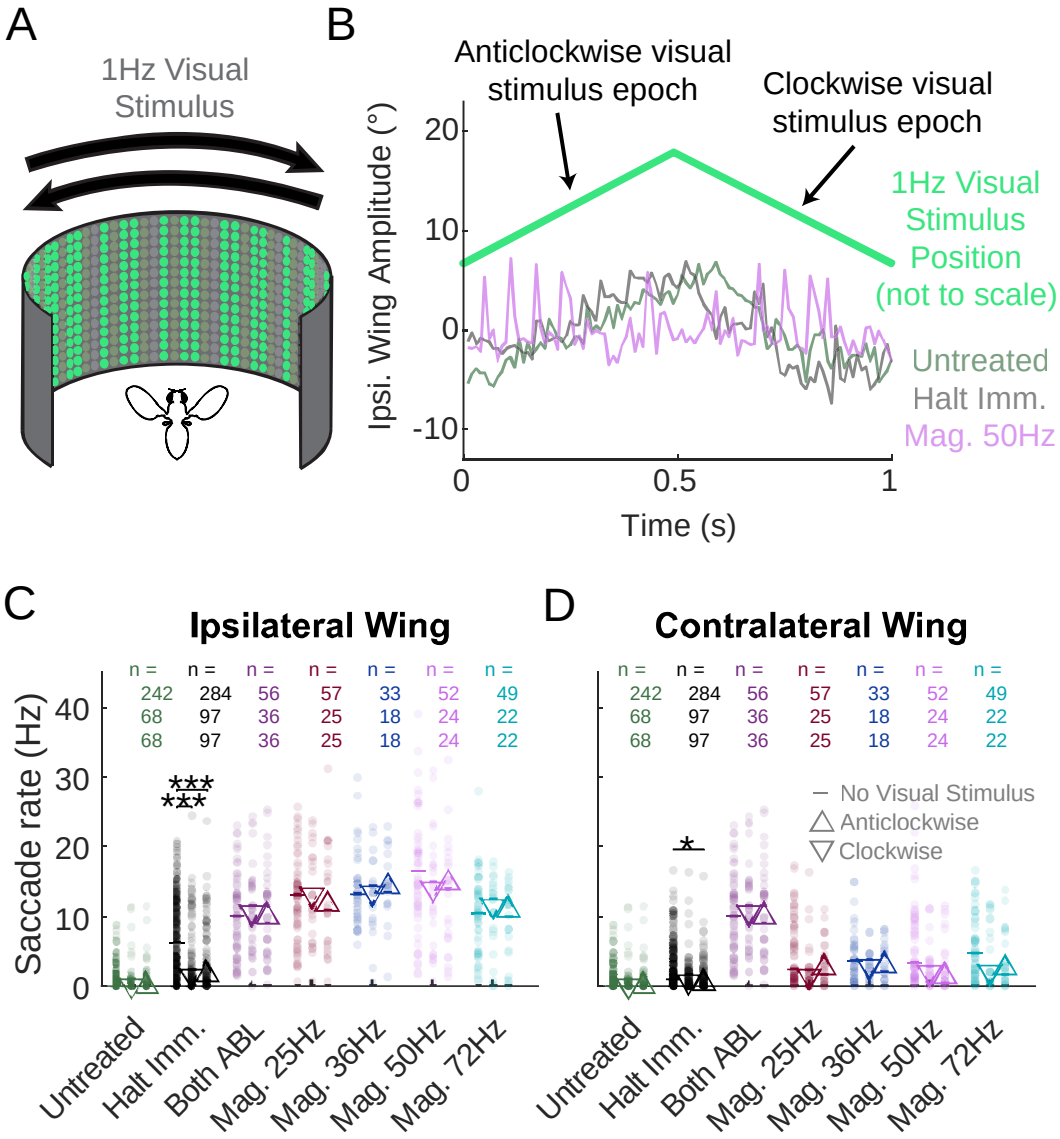


**Figure 4. Concurrent visual input does not influence saccade rate during most haltere manipulations** **(A)** Schematic of visual stimulus, showing irregular stripe pattern moving on an LED panel under the control of a 1Hz triangle-wave with a pattern velocity of 90°/s **(B)** Example ipsilateral wing amplitude responses to one cycle of the visual stimulus under several haltere treatment conditions. **(C)** Ipsilateral wing saccade rate across visual conditions, showing no change between uniform visual stimulus (reproduced from Fig. 2), clockwise visual stimulus epochs anticlockwise epochs in most haltere treatment conditions. Mean value for each visual stimulus condition represented by dash, upward pointing triangle, and downward pointing triangle respectively. **(D)** Same as a (C) but for contralateral wing saccade rate (*** = significance at 0.1% alpha level, multiple Bonferroni-corrected Wilcoxon rank-sum test) (D) Same as a (C) but for contralateral wing saccade rate. (* = significance at 5% alpha level, multiple Bonferroni-corrected Wilcoxon rank sum test)

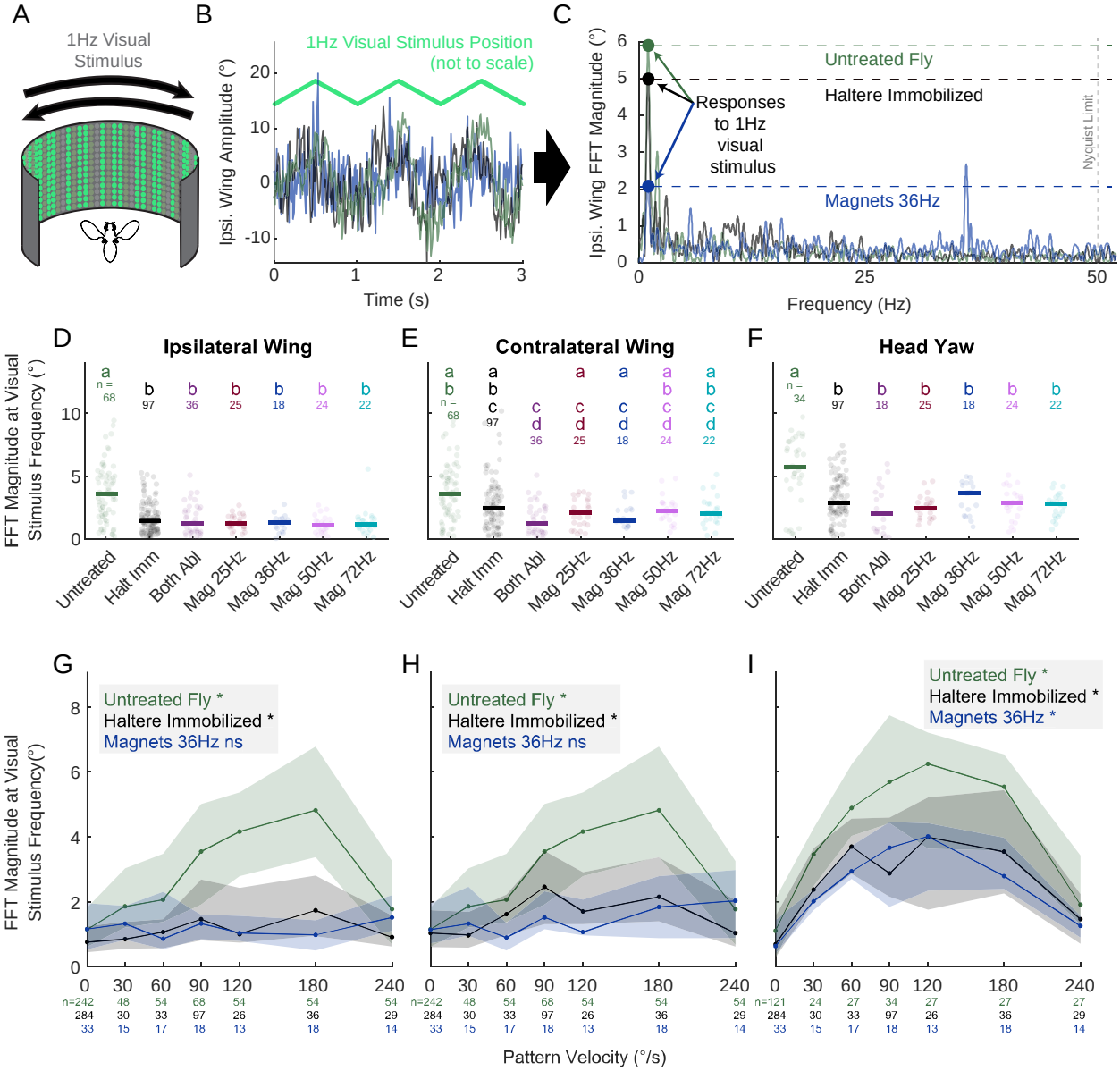


**Figure 5. Haltere manipulations influence visually-guided wing and head movements.**
**(A)** Schematic of visual stimulus, as in Fig. 4A **(B)** Example ipsilateral wing amplitude responses to multiple cycles of the visual stimulus under several haltere treatment conditions. **(C)** FFTs of traces from (B), showing peak at the frequency of the visual stimulus. **(D)** Ipsilateral wing response amplitude at visual stimulus frequency for all tested haltere treatments. For symmetrical manipulations (untreated, bilateral ablation), left and right wing responses are pooled. Letters denote statistical groupings from multiple Bonferroni-corrected Wilcoxon rank-sum test (5% alpha). **(E,F)** Same as (D) for contralateral wing and head yaw responses, respectively. Lines show median for each group. **(G)** Ipsilateral wing visual response magnitude, as estimated by measuring FFT magnitude at visual stimulus frequency, for untreated flies, haltere-immobilized flies, and 36Hz magnetic stimulation flies. Trendlines connect median data from each pattern velocity, with shaded region showing 1st and 3rd quartiles. Inset, results of Kruskal-Wallis omnibus test indicate whether pattern velocity is a significant predictor of response amplitude within each treatment group at the 5% alpha level (*) or not (ns). **(H-I)** Same as (G), but for contralateral wing and head yaw amplitude, respectively.